J|A|C|S
ARTICLES
Published on Web 03/06/2003

The Energy Landscape of Unsolvated Peptides: The Role of Context in the Stability of Alanine/Glycine Helices

Matthew R. Hartings, Brian S. Kinnear, and Martin F. Jarrold*

Contribution from the Chemistry Department, Indiana University, 800 East Kirkwood Avenue, Bloomington, Indiana 47405-7102

Received April 29, 2002; E-mail: mfj@indiana.edu

Abstract: Ion mobility measurements have been used to examine the conformations present for unsolvated Ac-$(AG)_7A+H^+$ and $(AG)_7A+H^+$ peptides (Ac = acetyl, A = alanine, and G = glycine) over a broad temperature range (100−410 K). The results are compared to those recently reported for Ac-$A_4G_7A_4+H^+$ and $A_4G_7A_4+H^+$, which have the same compositions but different sequences. Ac-$(AG)_7A+H^+$ shows less conformational diversity than Ac-$A_4G_7A_4+H^+$; it is much less helical than Ac-$A_4G_7A_4+H^+$ at the upper end of the temperature range studied, and at low temperatures, one of the two Ac-$A_4G_7A_4+H^+$ features assigned to helical conformations is missing for Ac-$(AG)_7A+H^+$. Molecular dynamics simulations suggest that the different conformational preferences are not due to differences in the stabilities of the helical states, but differences in the nonhelical states: it appears that Ac-$(AG)_7A+H^+$ is more flexible and able to adopt lower energy globular conformations (compact random looking three-dimensional structures) than Ac-$A_4G_7A_4+H^+$. The helix to globule transition that occurs for Ac-$(AG)_7A+H^+$ at around 250−350 K is not a direct (two-state) process, but a creeping transition that takes place through at least one and probably several intermediates.

Introduction

Understanding the factors that control the formation and stability of secondary structure is essential for a number of endeavors including the rational design of proteins. It is well known that some amino acids are better than others at making α-helices, and a considerable effort has been invested in determining helix propensities using both peptides and proteins.[1−11] A common approach is to make substitutions within a polypeptide and to determine their effect on the amount of helix present. However, the nature of the amino acids in a peptide is not the only factor that is important in determining whether it is helical. The sequence is also important, and certain amino acids have different propensities depending on their position along the polypeptide chain. For example, amino acids with positively charged side chains promote helix formation when they are located at the C-terminus because in this location they undergo favorable interactions with the helix macrodipole. For the same reason, negatively charged amino acids are better helix-makers when they are located at the N-terminus.[12−15] However, factors other than charge play a part in the sequence sensitivity. Another factor is context, which deals with how an amino acid interacts with its neighbors. For example, in an α-helix the *i* and *i*+4 residues can interact with each other. Two incompatible amino acids may destabilize a helix through this *i*,*i*+4 interaction, while two compatible ones may promote helix formation.

One of the first studies along these lines was performed by Baldwin and collaborators.[16] The C-peptide from RNase A is one of the few peptides that remains significantly helical in aqueous solution after removal from its parent protein. They found that interchanging His 12^+ with Ala 11 led to a substantial drop in helical content, which they attributed to a helix-stabilizing interaction between His 12^+ and Phe 8. Baldwin and collaborators have also studied short alanine-based peptides with a single glycine in the sequence. They found that the helix content decreased as the glycine was moved closer to the middle of the sequence.[17] Zou and Sugimoto have examined how the spacing and placement of single tryptophan and histidine residues in short alanine-based peptides cause a conformational switch between α-helix and β-sheet.[18] In related work, Santiveri

(1) Lyu, P. C.; Liff, M. I.; Marky, L. A.; Kallenbach, N. R. *Science* **1990**, *250*, 669−673.
(2) O'Neil, K. T.; DeGrado, W. F. *Science* **1990**, *250*, 646−651.
(3) Padmanabhan, S.; Marqusee, S.; Ridgeway, T.; Laue, T. M.; Baldwin, R. L. *Nature* **1990**, *344*, 268−270.
(4) Horovitz, A.; Matthews, J. M.; Fersht, A. R. *J. Mol. Biol.* **1992**, *227*, 560−568.
(5) Park, S. H.; Shalongo, W.; Stellwagen, E. *Biochemistry* **1993**, *32*, 7048−7053.
(6) Blaber, M.; Zhang, X. J.; Lindstrom, J. D.; Pepoit, S. D.; Baase, W. A.; Matthews, B. W. *J. Mol. Biol.* **1994**, *235*, 600−624.
(7) Chakrabartty, A.; Baldwin, R. L. *Adv. Protein Chem.* **1995**, *46*, 141−176.
(8) Munoz, V.; Serrano, L. *J. Mol. Biol.* **1995**, *245*, 275−296.
(9) Rohl, C. A.; Chakrabarrty, A.; Baldwin, R. L. *Protein Sci.* **1996**, *5*, 2623−2637.
(10) Yang, J.; Speck, El J.; Gong, Y.; Zhou, H.; Kallenbach, N. R. *Protein Sci.* **1997**, *6*, 1−9.
(11) Pace, C. N.; Scholtz, J. M. *Biophys. J.* **1998**, *75*, 422−427.
(12) Blagdon, D. E.; Goodman, M. *Biopolymers* **1975**, *14*, 241−245.
(13) Ihara, S.; Ooi, T.; Takahashi, S. *Biopolymers* **1982**, *21*, 131−145.
(14) Shoemaker, K. R.; Kim, P. S.; York, E. J.; Stewart, J. M.; Baldwin, R. L. *Nature* **1987**, *326*, 563−567.
(15) Daggett, V. D.; Kollman, P. A.; Kuntz, I. D. *Chem. Scr.* **1989**, *29A*, 205−215.
(16) Shoemaker, K. R.; Fairman, R.; Schultz, D. A.; Robertson, A. D.; York, E. J.; Stewart, J. M.; Baldwin, R. L. *Biopolymers* **1990**, *29*, 1−11.
(17) Chakrabartty, A.; Schellman, J. A.; Baldwin, R. L. *Nature* **1991**, *351*, 586−588.
(18) Zou, J.; Sugimoto, N. *J. Chem. Soc., Perkin Trans. 2* **2000**, 2135−2140.

et al. studied the stability of a β-hairpin with respect to the location of the β-turn using 15-residue peptides with the same composition but different sequences.[19]

In this article, we report studies of the conformations of unsolvated Ac-$(AG)_7A+H^+$ and $(AG)_7A+H^+$ over a wide temperature range (100−410 K). The results are compared to recent studies of the conformations of unsolvated Ac-$A_4G_7A_4+H^+$ and $A_4G_7A_4+H^+$, which have the same residues but different sequences.[20] This work is the first to examine the role of context in unsolvated peptides. It is part of a series of investigations of the energy landscape of unsolvated peptides that are sufficiently large that they can form secondary structure.[21−26] The motivation for these studies is to provide a better understanding of the intramolecular interactions responsible for protein folding. Studies of unsolvated peptides are the natural starting point for understanding their behavior across the range of environments that are important in biology, from aqueous solution to the hydrophobic interior of membranes. A number of different approaches have been used to examine the properties of unsolvated and partially solvated biological molecules in the vapor phase.[27−37]

In the work described here, unsolvated peptide ions are generated by electrospray, and information about their conformations is obtained from gas phase ion mobility measurements. The ion mobility depends on the average collision cross section, which in turn depends on the geometry.[38−40] Structural information is obtained by comparing the cross sections derived from the mobilities to cross sections calculated for trial geometries obtained from molecular dynamics (MD) simulations. This approach can easily distinguish the different conformations, like helices and globules (compact, random-looking, three-dimensional structures) that are commonly found for these peptides.[21]

The Ac-$(AG)_7A+H^+$ and Ac-$A_4G_7A_4+H^+$ peptides considered here were designed to have marginally stable helical states in the gas phase. Alanine has the highest helix propensity in aqueous solution, while glycine has one of the lowest.[1−3,7] Unsolvated alanine-based peptides form rigid helices in the gas phase,[22,23] while the glycine analogues form globules.[24] By mixing alanine and glycine residues the energy landscape is flattened so that helical and globular states have similar energies.[25] A variety of different conformations often coexist on the flattened energy landscape, and conformational changes including helix folding and unfolding transitions can be studied. In the present work, substantial differences, context effects, are found between the conformations of Ac-$(AG)_7A+H^+$ and Ac-$A_4G_7A_4+H^+$ peptides. MD simulations suggest that the different conformational preferences result primarily from differences in the relative energies of the globular conformations of these peptides. Lower energy globules result when the glycines and alanines are dispersed presumably because dispersing the glycines makes the peptide more flexible and able to adopt lower energy globular conformations.

Experimental Methods and Materials

Ac-$(AG)_7A$, and $(AG)_7A$ were synthesized using an Applied Biosystems Model 433A peptide synthesizer with *FastMoc* chemistry. The measurements were performed on a variable-temperature injected ion mobility apparatus, which has been described previously. The apparatus consists of an electrospray source with a heated capillary interface, a 30.48 cm long, variable-temperature drift tube, a quadrupole mass spectrometer, and a detector. Peptides were electrosprayed from solutions prepared by dissolving approximately 3 mg of peptide in 1 mL of trifluoracetic acid and 0.1 mL of water (the peptides studied here are very hydrophobic and insoluble in pure water and most other common solvents). Short pulses of electrosprayed ions are injected into the drift tube. The ions travel through the drift tube under the influence of a weak electric field and exit through a small aperture. The exiting ions are focused into a quadrupole mass spectrometer, and the arrival time distribution of the mass selected ions is recorded at the detector. The arrival time distribution is then corrected to give the drift time distribution (the time that the ions spend traveling across the drift tube) by accounting for the flight time outside the drift tube.

Experimental Results

Figure 1 shows drift time distributions recorded for Ac-$(AG)_7A+H^+$ with a range of drift tube temperatures. The points are the experimental data, and the lines are fits described below. At the lower temperatures ($\leq$293 K) there appear to be two peaks in the drift time distributions. However, a more detailed analysis performed by fitting the data with Gaussian functions[41] indicates that it is necessary to incorporate a third component to obtain a satisfactory fit to the measured distributions at and below 288 K. The third component is relatively small and lies between the two major peaks. It is responsible for the ledge that is evident between the peaks in the low-temperature distributions in Figure 1. Below 273 K the distributions remain, for the most part, unchanged. Above 273 K the peak at long drift time gradually collapses into the shorter drift time peak. The distributions between 288 and 313 K can be adequately fit using two Gaussians. Above 313 K a single Gaussian is sufficient to fit the drift time distributions for Ac-$(AG)_7A+H^+$.

As the ions are injected into the drift tube, they are collisionally heated as their kinetic energy is dissipated by collisions with the buffer gas. The transient heating cycle that occurs as the ions are injected into the drift tube can cause conformational changes.[42] However, there is no evidence of conformational

(19) Santiveri, C. M.; Rico, M.; Jiménez, M. A. *Protein Sci.* **2000**, *9*, 2151−2160.
(20) Kinnear, B. S.; Hartings, M. R.; Jarrold, M. F. *J. Am. Chem. Soc.* **2001**, *123*, 5660−5667.
(21) Hudgins, R. R.; Mao, Y.; Ratner, M. A.; Jarrold, M. F. *Biophys. J.* **1999**, *76*, 1591−1597.
(22) Hudgins, R. R.; Ratner, M. A.; Jarrold, M. F. *J. Am. Chem. Soc.* **1998**, *120*, 12974−12975.
(23) Hudgins, R. R.; Jarrold, M. F. *J. Am. Chem. Soc.* **1999**, *121*, 3494−3501.
(24) Hudgins, R. R.; Jarrold, M. F. J. *Phys. Chem. B* **2000**, *104*, 2154−2158.
(25) Kaleta, D. T.; Jarrold, M. F. *J. Phys. Chem. B* **2001**, *105*, 4436−4440.
(26) Kinnear, B. S.; Jarrold, M. F. *J. Am. Chem. Soc.* **2001**, *123*, 7907−7908.
(27) Jarrold, M. F. *Annu. Rev. Phys. Chem.* **2000**, *51*, 179−207.
(28) Suckau, D.; Shi, Y.; Beu, S. C.; Senko, M. W.; Quinn, J. P.; Wampler, F. M.; McLafferty, F. W. *Proc. Natl. Acad. Sci.* **1993**, *90*, 790−793.
(29) Campbell, S.; Rodgers, M. T.; Marzluff, E. M.; Beauchamp, J. L. *J. Am. Chem. Soc*. **1995**, *117*, 12840−12854.
(30) Schnier, P. D.; Price, W. D.; Jockusch, R. A.; Williams, E. R. *J. Am. Chem. Soc.* **1996**, *118*, 7178−7189.
(31) Kaltashov, I. A.; Fenselau, C. *Proteins: Struct. Func. Genet.* **1997**, *27*, 165−170.
(32) Valentine, S. J.; Clemmer, D. E. *J. Am. Chem. Soc.* **1997**, *119*, 3558−3566.
(33) Wyttenback, T.; Bushnell, J. E.; Bowers, M. T. *J. Am. Chem. Soc.* **1998**, *120*, 5098−5103.
(34) Arteca, G. A.; Velázquez, I.; Reimann, C. T.; Tapia, O. *Phys. Rev. E* **1999**, *59*, 5981−5986.
(35) Schaaff, T. G.; Stephenson, J. L.; McLuckey, S. L. *J Am. Chem. Soc.* **1999**, *121*, 8907−8919.
(36) Zwier, T. S. *J. Phys. Chem. A* **2001**, *105*, 8827−8839.
(37) Robertson, E. G.; Simons, J. P. *Phys. Chem. Chem. Phys.* **2001**, *3*, 1−18.
(38) Hagen, D. F. *Anal. Chem.* **1979**, *51*, 870−874.
(39) Von Helden, G.; Hsu, M.-T.; Kemper, P. R.; Bowers, M. T. *J. Chem. Phys.* **1991**, *95*, 3835−3837.
(40) Clemmer, D. E.; Jarrold, M. F. *J. Mass Spectrom.* **1997**, *32*, 577−592.
(41) The drift time distribution for a single isomer broadened by diffusion as the ions travel through the drift tube is expected to be a Gaussian.
(42) Jarrold, M. F.; Honea, E. C. *J. Phys. Chem.* **1991**, *95*, 9181−9185.

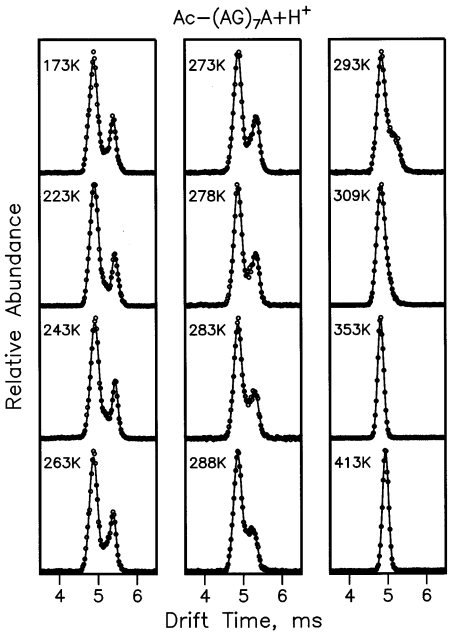

Figure 1. Drift time distributions measured for Ac-$(AG)_7A+H^+$ over the 100−410 K temperature range examined. The measurements were performed with an injection energy of 400 eV and a drift voltage of 380 V. The points are the experimental data, and the line is a fit using Gaussian functions (see text).

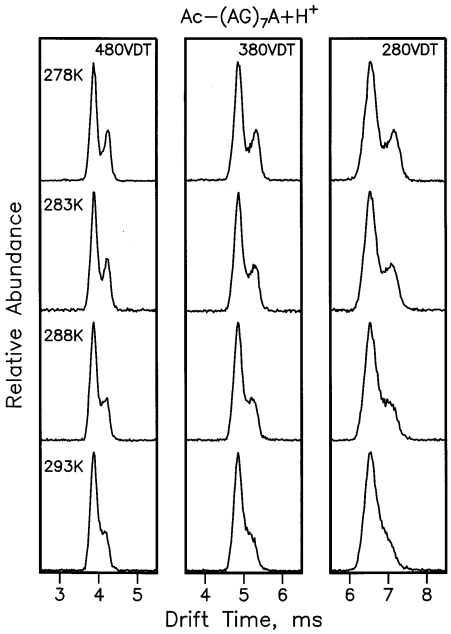

Figure 2. Drift time distributions measured for Ac-$(AG)_7A+H^+$ as a function of drift voltage in the temperature regime where the peak at long drift time is beginning to disappear (278−293 K).

changes for $(AG)_7A+H^+$ and Ac-$(AG)_7A+H^+$; the measured drift time distributions are virtually independent of the injection energy over the 300−600 eV range examined. The injection energy is required to overcome the buffer gas flow out of the drift tube apertures, and the signal drops off very sharply as the injection energy is dropped below 300 eV.

Figure 2 shows drift time distributions recorded as a function of drift voltage in the temperature regime where the drift time distribution is collapsing from two dominant peaks to a single peak (between 278 and 293 K). If ions enter the drift tube in two conformations (A and B) and one of the conformations (A) converts into the other (B) as they travel through the drift tube, this leads to a buildup of intensity between the peaks assigned to unreacted A and B. This intensity results from the reacting A ions spending part of their time in conformation A and part in conformation B. As the rate of interconversion increases, the intensity between the peaks increases until eventually the peak due to conformation A (the one that reacts) disappears as interconversion occurs rapidly compared to the drift time. This behavior is evident in the results shown in Figure 2. Decreasing the drift voltage increases the amount of time that the ions spend in the drift tube and hence provides more time for the ions to interconvert. As can be seen from Figure 2, as the drift time increases (the drift voltage decreases), the intensity between the two peaks increases and the feature at longer drift time becomes less well defined as more of it reacts away. These results provide unambiguous evidence that structural changes are occurring on the time scale of the drift time measurement. In previous work, we were able to fit the drift time distributions for the Ac-$(AGG)_5K+H^+$ peptide in the temperature range where conformational changes were occurring on the time scale of the drift time measurements and obtain rate constants for unfolding of the Ac-$(AGG)_5K+H^+$ α-helix into a globule.[20] A similar analysis was attempted here. While individual distributions could be closely fit using the same model that was used to analyze the Ac-$(AGG)_5K+H^+$ data, the Ac-$(AG)_7A+H^+$ distributions measured with the same temperature but different drift voltages (different reaction times) could not be fit with the same rate constant for unfolding of the helix into the globule. Satisfactory agreement could not even be achieved by incorporating a third unreactive component between the two peaks. The failure to fit the data with different reaction times with the same rate constant indicates that we are not dealing with a simple two-state system (where the helix converts directly into the globule). It is possible that the reaction involves an intermediate with a significant lifetime or that there are two or more different types of helix present which convert into globules with different rates.

The measured drift times are easily converted into collision cross sections.[43] Figure 3 shows a plot of the cross sections against temperature for the features identified for the Ac-$(AG)_7A+H^+$ and $(AG)_7A+H^+$ peptides. Only a single feature is observed in the drift time distributions for $(AG)_7A+H^+$ over the entire temperature range studied (98−413 K). The systematic decrease in the cross section for this feature with increasing temperature results because the long-range attractive interactions between the peptide ion and buffer gas become less important with increasing temperature and because the collisions become harder at higher temperature and ride further up the repulsive wall. This systematic decrease in the cross section with temperature always occurs, unless there is a conformational change that causes a significant increase in the cross section. A single feature like that found for $(AG)_7A+H^+$ is also observed for the $A_4G_7A_4+H^+$ peptide over a similar temperature range.[44] For $A_4G_7A_4+H^+$ this feature was assigned to a globular conformation. The cross sections for the $(AG)_7A+H^+$ peptide studied here are virtually identical, over the entire temperature range studied, to those previously determined for $A_4G_7A_4+H^+$.

(43) Mason, E. A.; McDaniel, E. W. *Transport Properties of Ions in Gases*; Wiley: New York, 1998
(44) Kinnear, B. S.; Hartings, M. R.; Jarrold, M. F. *J. Am. Chem. Soc.* **2002**, *124*, 4422−4431.

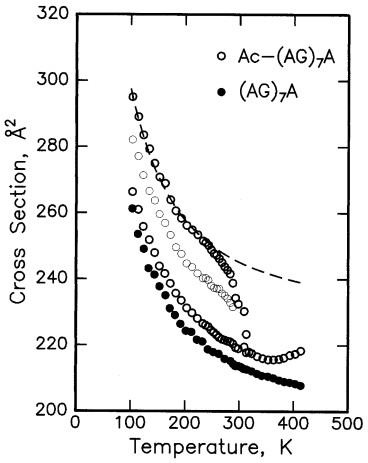

Figure 3. Plot of the cross sections for the main features in the drift time distributions for $(AG)_7A+H^+$ and Ac-$(AG)_7A+H^+$ as a function of drift tube temperature. The dashed line shows the expected temperature dependence, extrapolated from low temperature, of the Ac-$(AG)_7A+H^+$ feature with the largest cross sections. The dashed line was obtained by scaling the measured cross sections for $(AG)_7A+H^+$.

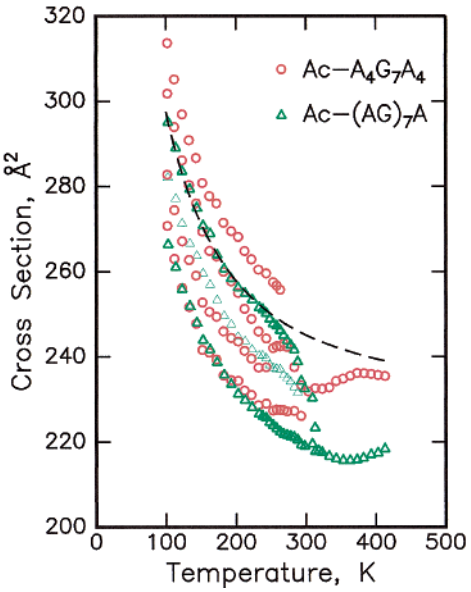

Figure 4. Comparison of the cross sections measured for Ac-$(AG)_7A+H^+$ (green points) and Ac-$A_4G_7A_4+H^+$ (red points) as a function of drift tube temperature.

This indicates that the $(AG)_7A+H^+$ peptide also adopts a globular conformation.

Cross sections for the Ac-$(AG)_7A+H^+$ peptide are shown as the open circles in Figure 3. As described above, there appear to be three conformations present at low temperatures for this peptide: the two peaks evident in the drift time distributions, and the small component between the two peaks revealed by fitting the data with Gaussian functions. The middle feature is plotted with lighter points in Figure 3 to represent its low relative abundance and the fact that it is not clearly evident in the drift time distributions as a peak. As the temperature increases, the Ac-$(AG)_7A+H^+$ feature with the largest cross section disappears, eventually merging, along with the small component in the middle, with the feature with the smallest cross section. The smallest set of cross sections for Ac-$(AG)_7A+H^+$ is close to the cross sections for the globular $(AG)_7A+H^+$ peptide. The small difference between these two sets of cross sections for temperatures < 350 K is due to the presence of the acetyl group in the Ac-$(AG)_7A+H^+$ peptide, which makes this peptide slightly larger than the unacetylated analogue. Thus for temperatures < 350 K the Ac-$(AG)_7A+H^+$ feature with the smallest cross section can be assigned to a globule. For higher temperatures the cross sections for the Ac-$(AG)_7A+H^+$ peptide increase with increasing temperature and move away from the cross sections for the $(AG)_7A+H^+$ globule. We will consider this behavior in more detail below.

Figure 4 shows a comparison of the cross sections reported here for the Ac-$(AG)_7A+H^+$ peptide to those obtained for Ac-$A_4G_7A_4+H^+$. The cross sections for the Ac-$A_4G_7A_4+H^+$ peptide shown in Figure 4 are slightly different from those reported previously by us because the data were originally analyzed manually and we have now reanalyzed them, fitting the distributions with Gaussian functions as described above for the Ac-$(AG)_7A+H^+$. This approach should allow a more accurate determination of the number of peaks in the drift time distributions and their positions, though for Ac-$A_4G_7A_4+H^+$ the differences were minor. As described previously, four features are evident in the drift time distributions for Ac-$A_4G_7A_4+H^+$ at 240 K and below. The features leading to the smallest and second smallest set of Ac-$A_4G_7A_4+H^+$ cross sections are only partially resolved from each other. In our previous work, the largest set of Ac-$A_4G_7A_4+H^+$ cross sections was assigned to an α-helix, the second largest set was assigned to a partial π-helix (conformations between an α-helix with 3.6 residues per turn and a π-helix with 4.4 residues per turn), the third largest (second smallest) was unassigned, and the smallest set of Ac-$A_4G_7A_4+H^+$ cross sections was assigned to a globule below 240 K. Above 240 K the cross sections for this feature increase and eventually merge with features with larger cross sections.

At low temperatures, below 240 K, the three sets of cross sections for the Ac-$(AG)_7A+H^+$ peptide match the first, second, and third smallest sets of cross sections for the Ac-$A_4G_7A_4+H^+$ peptide. There is no Ac-$(AG)_7A+H^+$ analogue for the largest set of cross sections for Ac-$A_4G_7A_4+H^+$. Evidently, the α-helical conformation is not formed or does not survive for Ac-$(AG)_7A+H^+$, though it does for Ac-$A_4G_7A_4+H^+$. The close correspondence between the three sets of cross sections for Ac-$(AG)_7A+H^+$ and those for the Ac-$A_4G_7A_4+H^+$ peptide suggests that the conformations present are closely related.

Molecular Dynamics Simulation

A series of molecular dynamics (MD) simulations were performed for the Ac-$(AG)_7A+H^+$ peptide to help interpret the experimental results presented above. The simulations were done using the MACSIMUS suite of programs,[45] with the CHARMM force field (21.3 parameter set),[46] and a dielectric constant of 1.0. The temperature was maintained by re-scaling the kinetic energies every 0.1 ps. Average potential energies and average collision cross sections were obtained from the final 35 ps of each simulation. Cross sections were calculated using an empirical correction to the exact hard spheres scattering model,[47]

(45) Kolafa, J. http://www.icpf.cas.cz/jiri/macsimus/default.htm.
(46) Brooks, B. R.; Bruccoleri, R. E.; Olafson, B. D.; States, D. J.; Swaminathan, S.; Karplus, M. *J. Comput. Chem.* **1983**, *4*, 187−217.
(47) Kinnear, B. S.; Kaleta, D. T.; Kohtani, M.; Hudgins, R. R.; Jarrold, M. F. *J. Am. Chem. Soc.* **2000**, *122*, 9243−9256.

averaging over 50 snapshots taken from the final 35 ps of each simulation. If the conformation is correct in the simulation, the calculated cross sections are expected to be within 2% of the measured values. The protonation site is assumed to be the amide CO nearest the C-terminus for all of the simulations. Protonation near the C-terminus is preferred for helical conformations because the charge then interacts favorably with the helix macrodipole.[12−15] Protonating an amide CO at the middle of the peptide or at the N-terminus disrupts the helix (MD simulations started from a helix rapidly convert into partially helical or globular conformation).[44] To survive in the simulations, a helix must be protonated near the C-terminus. For the globular conformations, it is not clear that there is a strong preference for protonation at a specific site along the backbone. The proton may even be mobile to some extent, transferring from one protonation site to another.[48,49] This behavior is not incorporated into the MD simulations. While we assume that the amide CO nearest the C-terminus is protonated, it is possible that one of the other protonation sites will lead to a lower energy globular conformation. This is a difficult issue to examine because of the problems in sampling the low-energy globules (see below).

The MD simulations described here are by necessity performed with a classical force field, and so the results should be interpreted with caution. The force field used here does not account for environment effects,[50] and it is not polarizable.[51] It may overemphasize some interactions, while other weak interactions, such as the $C^{\alpha}-H\cdots O{=}C$ hydrogen bond,[52] are missing. The Ac-$(AG)_7A+H^+$ and Ac-$A_4G_7A_4+H^+$ peptides have the same composition and protonation sites, and the main issue is whether there are significant differences in the MD results for the two peptides that might provide an explanation for their strikingly different conformational preferences. Normally, the force field energies of chemically different species cannot be compared. In the present case, however, we are dealing with sequence isomers and a comparison can be made.

The results of the MD simulations are summarized in Figure 5, which shows plots of the average potential energy against the cross section for Ac-$A_4G_7A_4+H^+$ (upper plot) and Ac-$(AG)_7A+H^+$ (lower plot). The results for Ac-$A_4G_7A_4+H^+$ were partly taken from our previous work on this peptide. In both cases three types of simulation were performed: 300 K 960 ps MD simulations starting from an ideal α-helix (represented by the green circles in Figure 5); simulated annealing starting from an ideal α-helix (represented by the red diamonds); and simulated annealing starting from an extended string (represented by the black squares). We employed a relatively gentle simulated annealing schedule consisting of 240 ps at 600, 500, and 400 K and 480 ps at 300 K. It is difficult to locate compact, low-energy globular conformations, and in previous work this annealing schedule seemed to be the most effective. All together 200 simulations (50 for each of the two types of simulations starting from a helix and 100 simulated annealing runs from a linear start) were run for both Ac-$A_4G_7A_4+H^+$ and Ac-$(AG)_7A+H^+$.

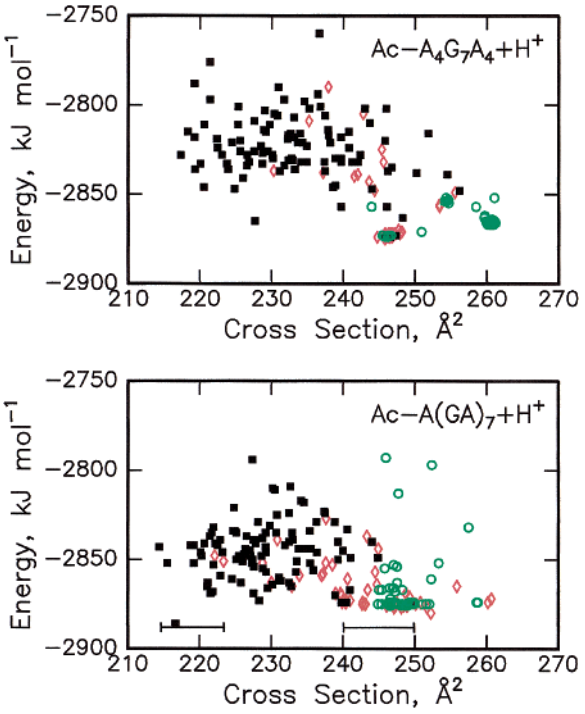

Figure 5. Plot of average potential energy against cross section from the MD simulations. Results are shown for Ac-$A_4G_7A_4+H^+$ (upper plot) and Ac-$(AG)_7A+H^+$ (lower plot). All results are from simulations that terminated at 300 K. Key: green circle = 960 ps 300 K MD simulation starting from ideal α-helix; red diamond = simulated annealing starting from ideal α-helix; black square = simulated annealing starting from a linear string (see text for more details). Cross sections for the two major features found in the drift time distributions of the Ac-$(AG)_7A+H^+$ peptide are represented by horizontal error bars toward the bottom of the figure. The error bars take into account the anticipated overall uncertainty of ±2% for comparison of the measured and calculated cross sections. The feature assigned to the Ac-$(AG)_7A+H^+$ globule is represented by the error bar centered at 219 Å^2. The Ac-$(AG)_7A+H^+$ helix is represented by the error bar centered at 245 Å^2. This value was extrapolated from lower temperature data (see Figure 3).

In the results of the simulations for Ac-$A_4G_7A_4+H^+$ (upper half of Figure 5) the group of points with energies around −2875 kJ mol^{-1} and cross sections around 246 Å^2 are partial π-helices (conformations between an α-helix with 3.6 residues per turn and a π-helix with 4.4 residues per turn). The group of points around 254 Å^2 and −2850 kJ mol^{-1} and those around 260 Å^2 and −2865 kJ mol^{-1} are both due to α-helices (they differ by the orientation of the protonated amide carbonyl group at the C-terminus). Low-energy conformations with cross sections smaller than 230 Å^2 are globules.

The results of the simulations for Ac-$(AG)_7A+H^+$ show some significant differences from those for Ac-$A_4G_7A_4+H^+$. The small cluster of Ac-$(AG)_7A+H^+$ points around 260 Å^2 and −2875 kJ mol^{-1} are α-helices. Despite their relatively low energy, only a few α-helices survive in the simulations for the Ac-$(AG)_7A+H^+$ peptide, substantially less survive than for Ac-$A_4G_7A_4+H^+$, and there is no analogue for the second slightly higher energy group of α-helices observed for Ac-$A_4G_7A_4+H^+$. Figure 6a shows an example of an Ac-$(AG)_7A+H^+$ α-helix. The C-terminus is twisted around so that the protonated amide carbonyl group can hydrogen bond to the dangling CO groups at the end of the helix (this is the lowest energy arrangement of

(48) Dongre, A. R.; Jones, J. L.; Somogyi, Á.; Wysocki, V. *J. Am. Chem. Soc.* **1996**, *118*, 8365−8374.
(49) Burlet, O.; Orkiszewski, R. S.; Ballard, K. D.; Gaskell, S. J. *Rapid Commun. Mass Spectrom.* **1992**, *6*, 658−662.
(50) Rick, S. W.; Cachau, R. E. *J. Chem. Phys.* **2000**, *112*, 5230−5241.
(51) Banks, J. L.; Kaminski, G. A.; Zhou, R. H.; Mainz, D. T.; Berne, B. J.; Friesner, R. A. *J. Chem. Phys.* **1999**, *110*, 741−754.
(52) Vargas, R.; Garza, J.; Dixon, D. A.; Hay, B. P. *J. Am. Chem. Soc.* **2000**, *122*, 4750−4755.

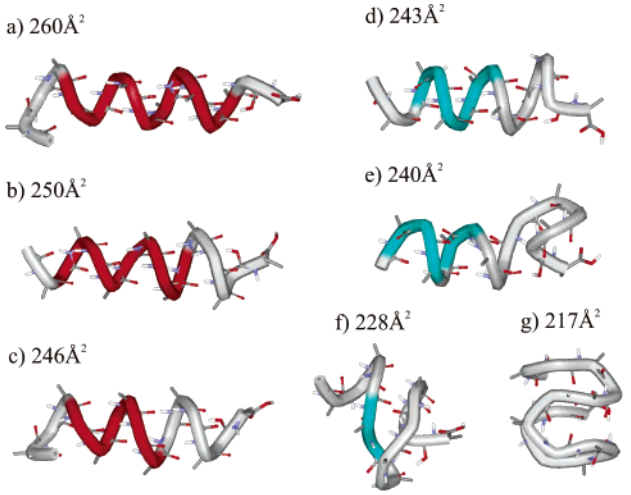

Figure 6. Examples of conformations found in the MD simulations. The conformations shown are snapshots from the end of the MD runs. Average energies and cross sections are (a) −2874 kJ mol^{-1}, 260 Å^2; (b) −2875 kJ mol^{-1}, 250 Å^2; (c) −2876 kJ mol^{-1}, 246 Å^2; (d) −2875 kJ mol^{-1}, 243 Å^2; (e) −2874 kJ mol^{-1}, 240 Å^2; (f) −2873 kJ mol^{-1}, 228 Å^2; and (g) −2886 kJ mol^{-1}, 217 Å^2. The individual images were generated by the WebLab Viewer (MSI Inc, San Diego, CA). Red regions are α-helical, and blue regions are β-sheet (on the basis of the backbone torsion angles Φ and Ψ).

the two orientations found for the Ac-$A_4G_7A_4$+H^+ peptide). The N-terminus of the α-helix is disordered. This disorder is a common feature of the simulations for Ac-$(AG)_7$A+H^+, much more so than for the Ac-$A_4G_7A_4$+H^+ peptide, presumably because the glycine residues are nearer the ends (glycine with no side chain has more conformational freedom than alanine).

The band of Ac-$(AG)_7$A+H^+ points with cross sections ranging from around 245 to 253 Å^2 and energies around −2875 kJ mol^{-1} are helices that are probably best described as partial π-helices. There is a fairly diverse range of different helical conformations present; generally they have more π-helical character closer to the C-terminus, and the N-terminus is often disordered. Two representative examples are shown in Figure 6b and c. The small cluster of points with cross sections around 243 Å^2 and energies around −2875 kJ mol^{-1} are also helices, but they have an unusual feature: a row of backward pointing hydrogen bonds (amide CO groups pointing toward the N-terminus and amide NH groups pointing toward the C-terminus). An example is shown in Figure 6d. The cluster of points with cross sections around 240 Å^2 and energies around −2875 kJ mol^{-1} are partial helices. An example is shown in Figure 6e. It is possible that the conformations shown in Figure 6d and e are intermediates in the unfolding of the α-helix or the partial π-helix to the globule. The lowest energy globular conformation (and the lowest energy conformation found in the simulations) is shown in Figure 6g. It has a double S-shaped structure that is very compact, with an average cross section of 217 Å^2. The next lowest energy globular conformation is shown in Figure 6f. It has an energy (−2873 kJ mol^{-1}) that is very close to the energies of the helices and an average cross section around 228 Å^2. This conformation, which looks like an unraveled helix, also might be an intermediate between the helical and globular conformations.

Discussion

For the unacetylated $(AG)_7$A+H^+ peptide only a single feature was observed in the drift time distribution, and this was assigned to a globule. For Ac-$(AG)_7$A+H^+ several conformations were observed, including one that was assigned to a globule. Similar behavior was found for $A_4G_7A_4$+H^+ and Ac-$A_4G_7A_4$+H^+. This difference in the conformations of the acetylated and unacetylated peptides can be attributed to the location of the protonation site. Acetylation blocks protonation at the N-terminus so that one of the amide CO groups must be protonated. For helical conformations protonation at an amide CO near the C-terminus is preferred because this leads to a favorable interaction between the charge and the helix macrodipole.[12−15] On the other hand, protonation near the N-terminus disrupts helix formation because there is an unfavorable interaction with the helix macrodipole. In the unacetylated peptides, the N-terminus is most likely protonated, disrupting helix formation. It follows that the N-terminus must be the most basic site in these peptides. While the N-terminus is known to be the most basic site in solution, the proton affinities of the N-terminus and backbone CO group are expected to be close in the absence of a solvent.[53] Studies of peptide dissociation have been interpreted as indicating that the protons are mobile.[48,49] However, the excess energy is probably a factor in driving the mobility of the protons in these studies, and it is reasonable to expect that the proton will be localized at room temperature if there is one site in the peptide that is more basic than all the others. Our results are consistent with the idea that the proton is localized near the N-terminus in the unacetylated peptide.

Two major features are observed for the Ac-$(AG)_7$A+H^+ peptide at low temperature (an additional minor feature was revealed by fitting the data). The major component with the smaller cross section is unambiguously assigned to the globule. The cross sections for the other major component are similar to those for the Ac-$A_4G_7A_4$+H^+ feature assigned to a partial π-helix. The cross section for this feature at 300 K, extrapolated from the lower temperature data (see dashed line in Figure 3), is around 245 Å^2. This value can be compared with the calculated cross sections shown in Figure 5; the horizontal error bar centered around 245 Å^2 takes into account the anticipated overall uncertainty of ±2% for comparison of the measured and calculated cross sections. Taking this uncertainty into account, the measured cross section is consistent with the partial π-helix represented by Figure 6c as well as the partially helical structures represented by Figure 6d. The partially helical structures represented by Figure 6e should also not be completely ruled out. The 300 K cross section for the globular conformation of the Ac-$(AG)_7$A+H^+ peptide is represented in Figure 5 by an error bar centered around 219 Å^2. The average cross section for the lowest energy globular conformation found in the simulations lies within the expected range. Only one compact low-energy conformation was found in the simulations, but as we have discussed elsewhere, it is not easy to find compact, low-energy globular conformations by MD even when it is coupled with simulated annealing.[54]

In the experiments, there is no Ac-$(AG)_7$A+H^+ analogue of the Ac-$A_4G_7A_4$+H^+ feature assigned to the α-helix. In the simulations, the Ac-$A_4G_7A_4$+H^+ helices are clustered into

(53) Rodriquez, C. F.; Cunje, A.; Shoeib, T.; Chu, I. K.; Hopkinson, A. C.; Siu, K. W. M. *J. Am. Chem. Soc.* **2001**, *123*, 3006−3012.
(54) Damsbo, M.; Kinnear, B. S.; Ruhoff, P. T.; Jarrold, M. F.; Ratner, M. A. An Evolutionary Computation Approach to Polypeptide Folding. *Proc. Natl. Acad. Sci. U.S.A.* (submitted).

several groups with fairly well-defined conformations, and the α-helix is around 10 kJ mol^{-1} above the lower energy partial π-helix. For Ac-$(AG)_7A+H^+$ the partial π-helices are spread over a wider range of cross sections, indicating more conformational flexibility than for the Ac-$A_4G_7A_4+H^+$ peptide. The ends of the Ac-$(AG)_7A+H^+$ peptides seem much more prone to partially unravel in the simulations than for Ac-$A_4G_7A_4+H^+$. For Ac-$(AG)_7A+H^+$ the α-helix and partial π-helices are almost isoenergetic in the simulations (see Figure 5). Despite this, the number of peptides that remain α-helical at the end of the simulations is much smaller for Ac-$(AG)_7A+H^+$ than for Ac-$A_4G_7A_4+H^+$. Two factors may contribute to this observation. First, the barriers for interconversion between different helical conformations may be lower for the Ac-$(AG)_7A+H^+$ peptide (less rough energy landscape), and second, the disorder in the partial π-helix/partially helical Ac-$(AG)_7A+H^+$ conformations makes them entropically preferred over the α-helix. These factors presumably account for the absence of the α-helical conformation for Ac-$(AG)_7A+H^+$ in the experiments.

At low temperature (<250 K) the different conformations present do not interconvert on the time scale of the drift time measurement. However, conformational changes occur as the temperature is raised. Between 250 and 350 K the Ac-$(AG)_7A+H^+$ helix converts into the globule (the minor component with a drift time between the helix and globule also disappears over this temperature range). As noted above, attempts to fit the experimental data using a simple two-state model were not successful, indicating that the helix unfolding transition is more complex. It is evident from Figure 3 that the cross sections for the helical conformation begin to creep toward the globule as the temperature is raised above 250 K. This suggests that the transition to the globular conformation occurs through a series of intermediates, possibly including the small component in the measured drift time distributions between the helix and globule at low temperature. In the results of the MD simulations there are a number of low-energy conformations between the helices and the globules that may be intermediates, for example, the partially helical structures shown in Figure 6d and e. The unraveled structure in Figure 6f might also be an intermediate.

Above room temperature, the conformational changes are beginning to occur rapidly on the time scale of the drift time measurement. If the peptides are interconverting rapidly between two conformations (helical and globular, for example), then the average cross section provides a measure of the time spent in each conformation. At slightly above room temperature, the cross sections for the Ac-$(AG)_7A+H^+$ peptide indicate that the preferred conformation is globular. The cross sections for the Ac-$A_4G_7A_4+H^+$ peptide in this temperature range are significantly larger than for Ac-$(AG)_7A+H^+$ (see Figure 4), suggesting a much larger average helical content. The origin of the larger average helical content for the Ac-$A_4G_7A_4+H^+$ peptide could be due to differences in the relative stabilities of the helices or to differences in the relative stabilities of the globules. In the results of the MD simulations (see Figure 5) it is evident that the Ac-$(AG)_7A+H^+$ helices have very slightly lower energies than the Ac-$A_4G_7A_4+H^+$ helices. So the origin of the different conformational preferences of the two peptides does not appear to result from enhanced stability of the Ac-$A_4G_7A_4+H^+$ helix, at least within the framework of the simulations. On the other hand, the globular conformation for the Ac-$(AG)_7A+H^+$ peptide seems to be lower in energy than the corresponding conformation for Ac-$A_4G_7A_4+H^+$. It is not just that a low-energy compact conformation was found in the MD simulations for Ac-$(AG)_7A+H^+$, overall the globular conformations seem lower in energy for Ac-$(AG)_7A+H^+$ than for Ac-$A_4G_7A_4+H^+$ (see Figure 5). Presumably, when the glycines are distributed throughout the peptide, it is more flexible and able to adopt lower energy conformations. Thus it is the stability of the globule, rather than the helices, that dictates the conformational preference: Ac-$A_4G_7A_4+H^+$ prefers a helical conformation more than Ac-$(AG)_7A+H^+$ because it makes less stable globules than Ac-$(AG)_7A+H^+$. An analogous conclusion was reached in studies of helix formation in Ac-X_nK+H^+ peptides with X = glycine, alanine, valine, and leucine and K = lysine. Here the relative energy of the globule was related to the size of the amino acid: small residues (like glycine) yield compact low-energy globules, while bulkier residues which pack less well (like valine) have high-energy globules. For the Ac-$(AG)_7A+H^+$ and Ac-$(AG)_7A+H^+$ peptides studied here, which have the same composition, the cause is more subtle: the lower energy globules result when the glycines and alanines are dispersed rather than together.

Above 350 K the cross sections for the Ac-$(AG)_7A+H^+$ peptide start to increase (see Figure 3). Cross sections for the $(AG)_7A+H^+$ peptide continue to decrease over the same temperature range; thus the increase in the cross sections for Ac-$(AG)_7A+H^+$ is not due to a nonspecific unfolding process (to a random coil). A similar increase in the cross sections for Ac-$A_4G_7A_4+H^+$ occurs above 300 K. An increase in the cross section (relative to that for the unacetylated peptide) suggests an increase in the helical content. Normally one expects the relative abundance of the ordered conformation to decrease as the temperature is raised. However, as we have pointed out previously, the globule is a compact conformation with a configurational entropy that is much less than for a random coil.[44] The increase in the relative abundance of the helical conformation may be due to the helix having a higher vibrational entropy than the globule, as predicted by some recent calculations.[55] It is evident from Figure 3 that we have just captured the beginning of the conformational change for the Ac-$(AG)_7A+H^+$ peptide. We are currently modifying our apparatus so that the measurements can be extended to higher temperatures.

Acknowledgment. We thank Jiri Kolafa for use of his MACSIMUS molecular modeling programs and for his helpful advice. We gratefully acknowledge the support of the National Institutes of Health.

JA020610U

(55) Ma, B.; Tsai, C.-J.; Nussinov, R. *Biophys. J.* **2000**, *79*, 2739−2753.